COMMUNICATION

Check for updates

An electrochemical Hofmann rearrangement on acrylamide copolymers†

Muzhao Wang and Paul Wilson (iD) *

The primary amide side-chain of acrylamide copolymers has been utilised as an isocyanate surrogate. The isocyanate is formed under mild conditions *via* an electrochemical Hofmann rearrangement resulting in the formation of *O*-alkyl carbamate side-chains in alcohol solvents. This represents a new strategy for the modification of amide-functionalised (co)polymers.

Carbamides (ureas), carbamates (urethanes), carbamothioates and amides are all functional groups consisting of a carbonyl group with an α-*N*-substituent. They are ubiquitous in nature while synthetic analogues are widely applied in medicinal chemistry and polymer/materials science.[1–5] These functional groups are typically accessed from carboxylic acids, or derivatives thereof, *via* isocyanate intermediates.[6]

In the context of polymer synthesis and functionalisation, the importance of isocyanates cannot be understated. For example, diisocyanates are required for the synthesis of polyureas and polyurethanes which have global market values in the region $1 billion and $75 billion USD respectively.[7,8] Isocyanates are also attractive intermediates for polymer functionalisation because they undergo clean addition reactions with amine,[9] alcohol[10] and thiol-based[11] nucleophiles with 100% atom economy. Despite this there are several limitations associated with the use of isocyanates. Traditional synthetic routes require multi-step reactions, employ hazardous reagents (*e.g.* azides, phosgene) and have poor overall atom economy.[12,13] Alternative strategies for generating isocyanates at polymer chain-ends and/or side-chains have been developed. The common strategy requires the incorporation of 'masked' isocyanates or isocyanate surrogates.[14–17] One prominent approach involves the incorporation of carbonyl-azide functional groups that can undergo a Curtius rearrangement forming isocyanates *in situ*.[18] This has been exploited for

polymer–polymer ligation,[19] polymer–peptide conjugation[20] and post-polymerisation modification.[21] Despite the efficiency of these reactions, it is still necessary to synthesise carbonylazide derivatives pre- or post-polymerisation.

The Hofmann rearrangement[22] provides access to isocyanates from primary amide precursors. The classical reaction employs stoichiometric amounts of halogen reagents in the presence of the NaOH resulting in highly corrosive and toxic reaction conditions. Alternative strategies employ stoichiometric amounts of iodine(III) or *N*-bromosuccinimide.[23–25]

Electrochemical intervention in (macro)molecular synthesis has received renewed interest over the last decade.[26–28] Through control of the electric field, the thermodynamics and/or kinetics of electron transfer processes and therefore reaction mechanisms can be precisely interrogated, controlled and understood.[29,30] Furthermore, the use of electrons as reagents, derived from sustainably generated power (solar, wind, water, *etc.*), represents a more environmentally-benign approach to synthesis compared to analogous chemically-driven processes.

The practical limitations associated with the Hofmann rearrangement have been overcome through the development of an electrochemical Hofmann (eHofmann) rearrangement. These methods replace stoichiometric halogens with catalytic halide salts (*e.g.* KBr, NaBr) and highly basic reaction media with neutral alcohol or mixed organic/alcohol solvent systems.[31,32] The halogen and base required to promote the formation of the isocyanate intermediate are generated *in situ* by anodic oxidation (halide to halogen) and cathodic reduction (alcohol to alkoxide). The most recent strategy employs constant current electrolysis in acetonitrile/MeOH at 50 °C, using 50 mol% NaBr as mediator in the absence of any other reagents or electrolytes. Under these conditions aryl and alkyl amides are converted to *O*-methyl carbamates in good yields.[33]

Herein, we build on our recent work on the electrochemically triggered/mediated synthesis of polymers (by eATRP)[34–37] by adopting the eHofmann rearrangement to achieve mild and efficient modification of acrylamide containing copolymer scaffolds for the first time. Overall we demonstrate that the

Department of Chemistry, University of Warwick, Coventry, CV4 7AL, UK.
E-mail: p.wilson.1@warwick.ac.uk

†Electronic supplementary information (ESI) available. See DOI: https://doi.org/10.1039/d3py00594a

primary amide side-chains can serve as 'masked' isocyanates which can be captured by alcohol-based nucleophiles forming O-alkyl carbamate side chains in the process.

Initially we adapted the reaction conditions reported to Zhang et al.[33] to reproduce the eHofmann rearrangement of benzamide using our electrosynthesis apparatus (see ESI, Fig. S1†). In an undivided cell equipped with graphite working and counter electrodes quantitative conversion of benzamide into the methyl N-phenyl carbamate was achieved in the presence of NaBr (50 mol%) in MeCN/MeOH (8 : 2 v/v) within 8 h at 60 °C under constant current electrolysis (CCE) at I_{app} = 50 mA (Table S1 and Fig. S2†).

With a view to applying this chemistry to acrylamide-containing copolymers, the eHofmann rearrangement of butyramide was attempted under the same conditions. Quantitative conversion to methyl N-propyl carbamate was achieved within 6 h (Table 1). The structure of the product was confirmed by ^{1}H NMR through the appearance of the O-methyl protons at δ_H = 3.65 ppm and a shift in the methylene protons (H_c) from δ_H = 2.35 to 3.12 ppm (Fig. S3†). Considering potential solubility issues of acrylamide copolymers in MeCN, the eHofmann rearrangement of butyramide was repeated in pure MeOH. Pleasingly, quantitative conversion to methyl N-propyl carbamate was achieved within 3 h (Table 1). Reducing the reaction temperature to 50 °C had little effect on conversion, however when the reaction was run at 40 °C the rate of reaction decreased with only 68% conversion achieved within 3 h. Reactions performed on acrylamide-containing (co)polymer scaffolds were subsequently performed at 60 °C.

Acrylamide-containing (co)polymer scaffolds were prepared via free radical polymerization (FRP) of acrylamide (Am) and dimethylacrylamide (DMAm) in MeOH targeting PAm and PDMAm homopolymers and P(Am-co-DMAm) copolymer scaffolds with Am feed ratios between 10–50 mol% (Table S2†). The chemical composition of all the polymers was determined by ^{1}H/^{13}C NMR in D_2O and Fourier-transform infra-red (FTIR) spectroscopy with comparison to PAm and PDMAm homopolymers. Using ^{1}H NMR (Fig. S4†), integration of the protons

corresponding to the N,N-dimethyl group of the DMAm side chain (δ_H = 2.78–3.15 ppm), against the entire copolymer backbone (δ_H = 1.19–2.77 ppm), with correction for the contribution to the backbone from DMAm, yielded Am compositional ratios of 7, 17 and 50 mol% (Table S3†). The ^{13}C NMR (Fig. S5†) and FTIR spectra (Fig. S6†) show two distinct C=O groups assigned to the amide groups of Am (δ_C = 180 ppm) and DMAm (δ_C = 176 ppm) side chains respectively. Molecular weight analysis performed using aqueous size exclusion chromatography (SEC, Fig. S7†) revealed the PAm homopolymer to have an $M_{n,SEC}$ = 7800 g mol^{-1} and $M_{w,SEC}$ = 38 000 g mol^{-1} (Table S3,† entry 5) whilst the PDMAm homopolymer had $M_{n,SEC}$ = 21 400 g mol^{-1} and $M_{w,SEC}$ = 71 700 g mol^{-1} (Table S3,† entry 1). The copolymer scaffolds gave comparable molecular weights with $M_{n,SEC}$ = between 13 700–20 000 g mol^{-1} and $M_{w,SEC}$ = between 71 200–78 800 g mol^{-1} (Table S3,† entries 2–4).
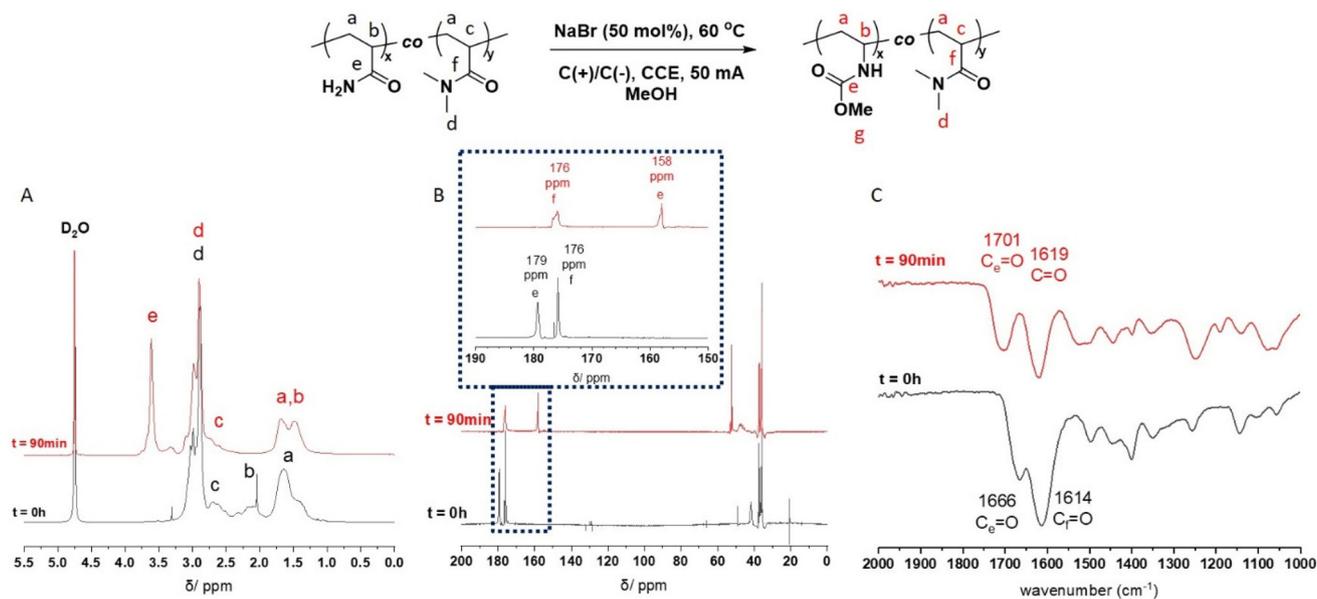
Thermogravimetric analysis (TGA) of PAm revealed thermal events occurring with onset temperatures of the 278 °C and 384 °C (Fig. S8A†). Conversely, PDMAm exhibited a single thermal event with an onset temperature of 417 °C (Fig. S8B†). Both degradation profiles were consistent with literature on PAm and N-disubstituted acrylamides.[38,39] The P(Am-co-DMAm) copolymers exhibited a two-step degradation profile expected for the proposed copolymer structure (Fig. S9†). Using differential scanning calorimetry (DSC) the glass transition temperatures (T_g) of PAm and PDMAm were found to be 194 °C and 125 °C respectively. For the P(Am-co-DMAm) scaffolds a single T_g was measured, supporting the targeted statistical composition of the polymers synthesised by FRP (Fig. S10†). The T_g increased with increasing mole fraction of Am. At the lowest mole fraction (7 mol%) the T_g = 140 °C which increased up to T_g = 178 °C for P(Am-co-DMAm) containing 50 mol% Am.

The P(Am-co-DMAm) scaffolds were then subjected to the conditions for eHofmann rearrangement. The scaffolds were dissolved in MeOH (1 mmol w.r.t. Am) and electrolysed via CCE at 50 mA in an undivided cell fitted with graphite working and counter electrodes with heating at 60 °C for 90 min. Structural analysis by ^{1}H NMR revealed a significant change in the region of the polymer backbone (Fig. 1A). The broad peak at δ_H = 2.25 ppm of the PAm backbone was completely absent and the pattern of the peaks at δ_H = 1.50–1.70 ppm changed. Furthermore there was a new peak at δ_H = 3.62 ppm which was assigned to the O-methyl group of the new carbamate side chain. Integration of this peak against the N,N-dimethyl group of the DMAm side chain (δ_H = 2.78–3.15 ppm) reveals quantitative conversion of the amide side chains to carbamate side chains. These structural changes are supported by ^{13}C NMR which shows a shift in the C=O carbon of the Am side from δ_C = 180 ppm in P(Am-co-DMAm) to δ_C = 158 ppm in the rearrangement product as well as appearance of the O-methyl carbon at δ_C = 53 ppm. The C=O signal from DMAm side chains is retained at δ_C = 176 ppm (Fig. 1B). Furthermore, FTIR of the scaffolds after rearrangement indicated retention of the DMAm derived C=O at 1614 cm^{-1} whilst the C=O

Table 1 ^{1}H NMR reaction monitoring of the eHofmann reaction of butyramide (1 mmol) under constant current electrolysis (CCE) at 50 mA with graphite working and counter electrodes

| Time (h)	Conv. (%) MeCN/MeOH = 8 : 2	Conv. (%) MeOH 60 °C	Conv. (%) MeOH 50 °C	Conv. (%) MeOH 40 °C
0	0	0	0	0
1	14	36	21	15
2	20	77	62	44
3	36	>99	97	68
4	58			
5	84			
6	99			

Fig. 1 Representative ^{1}H NMR (A), ^{13}C NMR (B) in D_2O and (C) FTIR showing the carbonyl region confirms quantitative conversion of the acrylamide side-chain to the *O*-methyl carbamate side chain using P(Am-*co*-DMAm) scaffold containing 50 mol% Am.

derived from the Am side chain (1660 cm^{-1}) shifted completely to 1700 cm^{-1}, indicative of carbamate formation (Fig. 1C).

Molecular weight analysis by aqueous SEC indicated that the eHofmann rearrangement proceeded with a small decrease in molecular weight (Table S4 and Fig. S11†). Molecular weight analysis of the P(Am-*co*-DMAm) scaffolds and rearrangement productions was repeated using DMF GPC. The P(Am-*co*-DMAm) scaffold containing 50 mol% Am was not soluble in DMF. However the scaffolds contain 7 and 17 mol% Am gave $M_{n,SEC}$ values of 39 200 g mol^{-1} ($Đ_m$ = 3.5) and 38 500 g mol^{-1} ($Đ_m$ = 3.3) respectively. The formation of the *O*-methyl carbamate rearrangement products resulted in an increase in molecular weight and little change in the dispersity (Table 2 and Fig. 2). Furthermore, whilst the P(Am-*co*-DMAm) scaffold containing 50 mol% Am was not soluble in DMF, the *O*-methyl carbamate rearrangement product derived from this scaffold was soluble with $M_{n,SEC}$ = 36 700 g mol^{-1} and $Đ_m$ = 3.3.

The effect of converting the pendant amide groups into carbamates on the thermal properties of the copolymer scaffolds was explored by TGA and DSC. Methyl *N*-alkyl/aryl carbamates are known to undergo thermal decomposition *via* competing
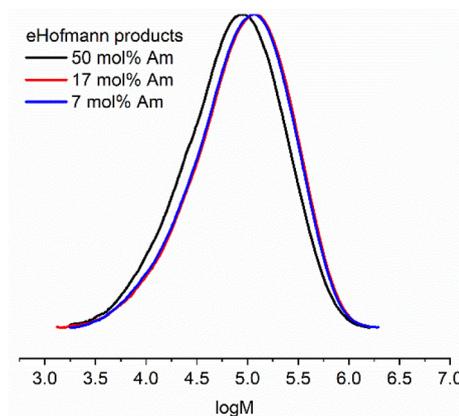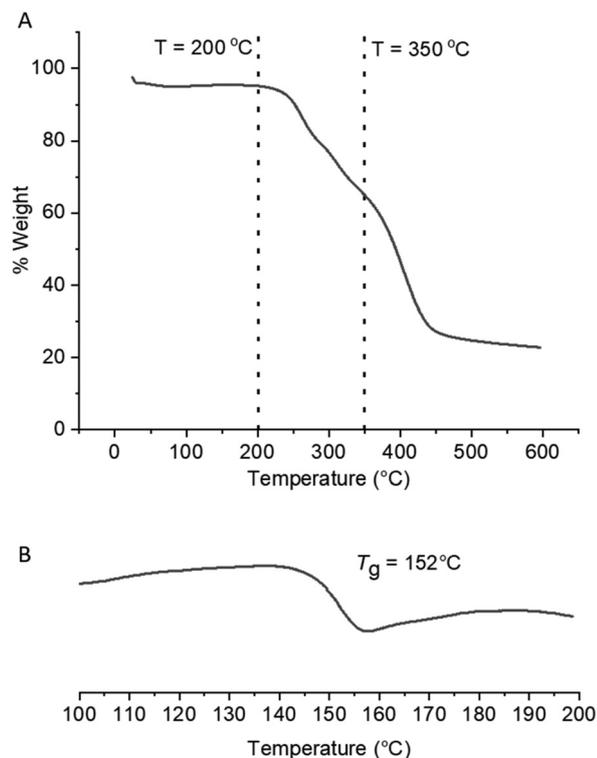

Fig. 2 Molecular weight distributions from DMF SEC of the *O*-methyl carbamate functionalised polymer products formed *via* eHofmann rearrangement (Table 2).

pathways, one of which involves elimination of MeOH and formation of alkyl/aryl isocyanates, the proposed intermediate of the forward eHofmann reaction.[40–44] The methyl carbamate-DMAm copolymers were shown to have different degradation profiles to the parent P(Am-*co*-DMAm) scaffolds by TGA (Fig. S9†), exhibited three meaningful thermal events (Fig. 3A). The two thermal events that occur at lower temperatures ($T_{d,onset}$ = 205–250 °C) can be attributed to decomposition of the *O*-methyl carbamate side chain. The higher temperature event (T > 330 °C) relates to degradation of the remaining polymer. Likewise, DSC revealed that the T_g of the *O*-methyl carbamate copolymers was lower than the parent P(Am-*co*-DMAm) scaffolds which is attributed to the relative hydrogen bonding ability of the primary amide and carbamate side chains respectively (Table S5,† Fig. 3B and S12–14†).

Table 2 Molecular weight data for the P(Am-*co*-DMAm) scaffolds and rearrangement productions from DMF SEC

| Am (mol%)	P(Am-*co*-DMAm)		eHofmann product	
	$M_{n,SEC}$ (g mol^{-1})	$Đ_m$	$M_{n,SEC}$ (g mol^{-1})	$Đ_m$
7	39 200	3.5	45 200	3.2
17	38 500	3.3	45 300	3.3
50	—	—	36 700	3.3

Fig. 3 For the *O*-methyl carbamate functionalised polymer product derived from P(Am-*co*-DMAm) containing 50 mol% Am; (A) TGA analysis showing two thermal events occurring between T = 200–350 °C and a third event at T > 350 °C; (B) DSC analysis showing that T_g = 152 °C, decreasing from 178 °C following eHofmann rearrangement (Fig. S14†).

From a mechanistic point of view, cyclic voltammetry (CV) was performed to confirm that the P(Am-*co*-DMAm) scaffolds in MeOH were not redox active (Fig. S15†). Upon addition of NaBr (50 mol%) a significant anodic current was observed which is consistent with the reactions performed on small molecule substrates and can be attributed to the oxidation of bromide. Thus, with reference to the mechanism proposed by Zhang *et al.*[33] we hypothesise that bromine formed *via* oxidation of bromide is captured by the Am side chains forming *N*-bromoamide intermediates. At the cathode, reduction of MeOH forming MeO⁻ and H₂ generates the base required to trigger rearrangement of the *N*-bromoamide to an isocyanate which subsequently reacts with MeO⁻ to yield the *O*-methyl carbamate product (Fig. 4).

Finally, the P(Am-*co*-DMAm) scaffold containing 50 mol% Am was subjected to the conditions for eHofmann rearrangement using diethylene glycol monomethyl ether (DEGME) as alternative alcohol solvent. The reaction was performed with the same electrochemical cell configuration. The loading of NaBr was increase (400 mol%) and the reaction temperature was increased to 90 °C to ensure full dissolution of the P(Am-*co*-DMAm) scaffolds and sufficient charging of the system. Pleasingly, the reaction reached near quantitative conversion in 4 h (Fig. S16†). Formation of the *O*-DEGME carbamate side chains was confirmed by ¹H/¹³C and FTIR spectroscopy
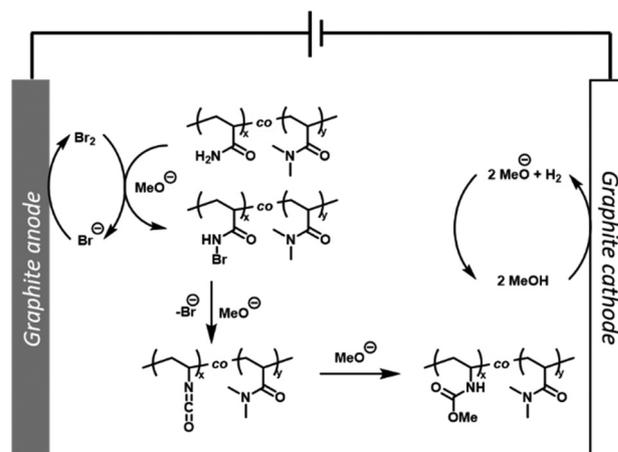
Fig. 4 Proposed mechanism for the eHofmann rearrangement on P(Am-*co*-DMAm) scaffolds.

(Fig. S16–S18†). Likewise, the thermal properties of the *O*-DEGME carbamate-DMAm copolymers confirmed changes to the copolymer structure. TGA revealed a 2-step degradation profile with an onset temperature of T_d = 225 °C (Fig. S19A†) while DSC revealed an expected decrease in T_g (87 °C, Fig. S19B†) relative to the parent P(Am-*co*-DMAm) scaffold (Fig. S10†).

In conclusion, an efficient electrochemical method for the rearrangement of the primary amide side-chain, present in Am-containing polymers, to an *O*-methyl carbamate side-chain in the presence of MeOH has been developed. A simple, undivided electrochemical cell configuration containing non-noble metal electrodes (graphite) and NaBr (50 mol%) under CCE at 50 mA was sufficient to drive an eHofmann rearrangement on P(Am-*co*-DMAm) scaffolds containing 7–50 mol% Am side chains. The success of the reactions was determined by quantitative conversion of the amide side chains to carbamates according to ¹H/¹³C and FTIR spectroscopy. Furthermore, the rearrangement from amide to carbamate side chains was confirmed by changes in the thermal properties of the resulting carbamate-functionalised copolymers. The reaction is compatible with other alcohol solvents, exemplified by formation of *O*-DEGME carbamate containing copolymers when reactions were performed in DEGME. This represents the first report of an eHofmann reaction for the functionalisation of Am-containing polymers. Crucially, the amide plays the role of a 'masked' isocyanate which through electrochemical intervention can be accessed in the absence of the hazardous reagents such as phosgene. At this stage the scope and limitation of the eHofmann rearrangement in polymer synthesis and functionalisation is unknown and under investigation in our team. These preliminary results allude to the potential of this chemistry as a platform to synthesise and characterise alkyl/aryl-*N*-vinyl carbamate functionalised (co)polymers which are synthetically challenging by other routes and as a result have received limited attention in the field up to now.[45,46] Alternative nucleophilic reacting partners including amines

and thiols are also being explored as potential routes to urea and carbamothioate functionalised (co)polymers respectively. Furthermore, by exploiting the control enabled by reversible deactivation radical polymerization (RDRP), the potential of incorporating these functional groups into more complex (co)polymer compositions and architectures is also being investigated.

Conflicts of interest

There are no conflicts to declare.

Acknowledgements

References

1 J. O. Akindoyo, M. D. H. Beg, S. Ghazali, M. R. Islam, N. Jeyaratnam and A. R. Yuvaraj, *RSC Adv.*, 2016, **6**, 114453–114482.

2 J. Kozakiewicz, G. Rokicki, J. Przybylski, K. Sylwestrzak, P. G. Parzuchowski and K. M. Tomczyk, *Polym. Degrad. Stab.*, 2010, **95**, 2413–2420.

3 A. M. C. Maan, A. H. Hofman, W. M. de Vos and M. Kamperman, *Adv. Funct. Mater.*, 2020, **30**, 2000936.

4 F. Xie, T. Zhang, P. Bryant, V. Kurusingal, J. M. Colwell and B. Laycock, *Prog. Polym. Sci.*, 2019, **90**, 211–268.

5 A. K. Ghosh and M. Brindisi, *J. Med. Chem.*, 2015, **58**, 2895–2940.

6 R. Ahmed, R. Gupta, Z. Akhter, M. Kumar and P. P. Singh, *Org. Biomol. Chem.*, 2022, **20**, 4942–4948.

7 https://www.grandviewresearch.com/industry-analysis/polyurethane-pu-market (accessed 25/5/2023).

8 https://www.grandviewresearch.com/industry-analysis/polyurea-market, (accessed 25/5/2023).

9 J. Yoon and P. A. Lovell, *Macromol. Chem. Phys.*, 2008, **209**, 279–289.

10 J. D. Flores, N. J. Treat, A. W. York and C. L. McCormick, *Polym. Chem.*, 2011, **2**, 1976–1985.

11 R. M. Hensarling, S. B. Rahane, A. P. LeBlanc, B. J. Sparks, E. M. White, J. Locklin and D. L. Patton, *Polym. Chem.*, 2011, **2**, 88–90.

12 H. Lebel and O. Leogane, *Org. Lett.*, 2005, **7**, 4107–4110.

13 H. Babad and A. G. Zeiler, *Chem. Rev.*, 1973, **73**, 75–91.

14 M. S. Rolph, M. Inam and R. K. O'Reilly, *Polym. Chem.*, 2017, **8**, 7229–7239.

15 M. S. Rolph, A. L. J. Markowska, C. N. Warriner and R. K. O'Reilly, *Polym. Chem.*, 2016, **7**, 7351–7364.

16 W. Liu, S. Yang, L. Huang, J. Xu and N. Zhao, *Chem. Commun.*, 2022, **58**, 12399–12417.

17 A. Petti, C. Fagnan, C. G. W. van Melis, N. Tanbouza, A. D. Garcia, A. Mastrodonato, M. C. Leech, I. C. A. Goodall, A. P. Dobbs, T. Ollevier and K. Lam, *Org. Process Res. Dev.*, 2021, **25**, 2614–2621.

18 A. K. Ghosh, A. Sarkar and M. Brindisi, *Org. Biomol. Chem.*, 2018, **16**, 2006–2027.

19 J. C. Brendel, G. Gody and S. Perrier, *Polym. Chem.*, 2016, **7**, 5536–5543.

20 G. Gody, D. A. Roberts, T. Maschmeyer and S. Perrier, *J. Am. Chem. Soc.*, 2016, **138**, 4061–4068.

21 G. Gody, C. Rossner, J. Moraes, P. Vana, T. Maschmeyer and S. Perrier, *J. Am. Chem. Soc.*, 2012, **134**, 12596–12603.

22 H. E. Baumgarten and A. Staklis, *J. Am. Chem. Soc.*, 1965, **87**, 1141–1142.

23 N. Satoh, T. Akiba, S. Yokoshima and T. Fukuyama, *Tetrahedron*, 2009, **65**, 3239–3245.

24 M. Iinuma, K. Moriyama and H. Togo, *Tetrahedron*, 2013, **69**, 2961–2970.

25 X. Huang, M. Seid and J. W. Keillor, *J. Org. Chem.*, 1997, **62**, 7495–7496.

26 S. D. Minteer and P. Baran, *Acc. Chem. Res.*, 2020, **53**, 545–546.

27 C. Schotten, T. P. Nicholls, R. A. Bourne, N. Kapur, B. N. Nguyen and C. E. Willans, *Green Chem.*, 2020, **22**, 3358–3375.

28 B. Zhao and P. Wilson, *Polym. Chem.*, 2023, **14**, 2000–2021.

29 K. D. Moeller, *Chem. Rev.*, 2018, **118**, 4817–4833.

30 C. Sandford, M. A. Edwards, K. J. Klunder, D. P. Hickey, M. Li, K. Barman, M. S. Sigman, H. S. White and S. D. Minteer, *Chem. Sci.*, 2019, **10**, 6404–6422.

31 S. Tatsuya, M. Yoshihiro, Y. Shin-ichiro and K. Shigenori, *Chem. Lett.*, 1982, **11**, 565–568.

32 Y. Matsumura, T. Maki and Y. Satoh, *Tetrahedron Lett.*, 1997, **38**, 8879–8882.

33 L. Li, M. Xue, X. Yan, W. Liu, K. Xu and S. Zhang, *Org. Biomol. Chem.*, 2018, **16**, 4615–4618.

34 B. Zhao, J. Cheng, J. Gao, D. M. Haddleton and P. Wilson, *Macromol. Chem. Phys.*, 2023, 2300039.

35 M. Mohammed, B. A. Jones and P. Wilson, *Polym. Chem.*, 2022, **13**, 3460–3470.

36 B. Zhao, F. Pashley-Johnson, B. A. Jones and P. Wilson, *Chem. Sci.*, 2022, **13**, 5741–5749.

37 B. Zhao, M. Mohammed, B. A. Jones and P. Wilson, *Chem. Commun.*, 2021, **57**, 3897–3900.

38 M. E. S. R. e. Silva, E. R. Dutra, V. Mano and J. C. Machado, *Polym. Degrad. Stab.*, 2000, **67**, 491–495.

39 M. J. Caulfield, G. G. Qiao and D. H. Solomon, *Chem. Rev.*, 2002, **102**, 3067–3084.

40 N. J. Daly and F. Ziolkowski, *Int. J. Chem. Kinet.*, 1980, **12**, 241–252.

41 N. J. Daly, G. Heweston and F. Ziolkowski, *Aust. J. Chem.*, 1973, **26**, 1259–1262.

42 N. Daly and F. Ziolkowski, *Aust. J. Chem.*, 1972, **25**, 1453–1458.

43 N. Daly and F. Ziolkowski, *Aust. J. Chem.*, 1971, **24**, 2541–2546.

44 C. E. Schweitzer, US2409712A, 1944.

45 L. J. Guilbault and H. J. Harwood, *J. Polym. Sci., Polym. Chem. Ed.*, 1974, **12**, 1461–1467.

46 G. O. Schulz and H. J. Harwood, *J. Polym. Sci., Polym. Chem. Ed.*, 1974, **12**, 1451–1460.